JOURNAL OF CATALYSIS 110, 171–183 (1988)

The Mechanism of Neopentane Cracking over Solid Acids

E. A. LOMBARDO,[1] R. PIERANTOZZI,[2] AND W. KEITH HALL[3]

Department of Chemistry, University of Pittsburgh, Pittsburgh, Pennsylvania 15260

Received June 16, 1987; revised October 26, 1987

Neopentane was used as a probe to test whether catalyst protons can attack the C–C and/or the C–H σ-bonds in the cracking of alkanes. Over a variety of solid acids approximately one CH_4 molecule was formed for every neopentane reacted. Moreover, in most cases nearly as much isobutene was formed. With H–Y zeolite (H–Y) and particularly with H–mordenite (H–M), however, hydride transfer leading to paraffin formation became important or dominant. Generally, the results conformed to

$$(CH_3)_3C\text{—}\underset{\underset{H^+}{|}}{\diagdown\diagup}\text{—}CH_3 \rightarrow CH_4 + (CH_3)_3C^+$$

with the *t*-butyl ion either decomposing to isobutene or else undergoing secondary reactions. The latter tended to increase with the intensive factor of the acidity, i.e., with the strength of the acid–base interaction. The fraction of neopentane converted to CH_4, when plotted in the Arrhenius fashion against T^{-1}, produced straight lines from which apparent activation energies could be calculated. Values obtained fell between 30 kcal/mol for silica–alumina and 14 kcal/mol for H–M (the most acidic and active catalyst investigated). Controversial views found in current literature are discussed in light of the present results.

INTRODUCTION

The acid catalyzed cracking of petroleum is by far the largest volume and most important industrial process in operation today. The mechanistic aspects of paraffin cracking over amorphous solid acids were first delineated by Greensfelder *et al.* (*1*) and have been further expanded and clarified by many others. Authoritative reviews may be found in a number of books, most recently in Refs. (*2*) and (*3*). It is generally accepted that the propagation steps of the carbenium ion chain mechanism postulated for catalytic cracking include a hydrogen (hydride) transfer step followed by β-scission (*1–3*),

$$RH + R_s^+ \rightarrow R^+ + R_sH \quad \text{(H-transfer)} \quad (1)$$

$$R^+ \rightarrow Ol + R_s^+ \quad (\beta\text{-scission}) \quad (2)$$

where RH is the reactant paraffin, R_s^+ a carbenium ion smaller than R^+, and *Ol* an olefin. Reaction (2) proceeds by β-scission; this cannot occur with the *t*-butyl or smaller ions.

One controversial aspect of the cracking of paraffins over solid acids concerns the nature of the initiation step, i.e., how the first carbenium ions are formed to start the chain process represented by Eqs. (1) and (2). Another related question concerns the possibility of a second cracking pathway which may coexist with Reaction (2) on solid acids, viz., the protolysis of the C–C bond. Consider

$$(R_i)_3C\text{–}C(R_j)_3 + H^+ \rightarrow (R_i)_3C\underset{\underset{H^+}{|}}{\diagdown\diagup}C(R_j)_3 \rightarrow (R_i)_3CH + (R_j)_3C^+ \quad (3a)$$

where R_i and R_j may represent both alkyl groups and hydrogen atoms. Note that the

[1] Permanent address: INCAPE, Sgo del Estero 2829, (3000) Santa Fe, Argentina.

[2] Air Products and Chemicals, Inc., Allentown, PA 18105.

[3] To whom all correspondence should be addressed.

0021-9517/88 $3.00

proton attack may be presumed to be at the most nucleophilic center, viz. the electrons of the C–C bond. Protolysis may also occur at a C–H bond where the intermediate species is typically written as a pentacoordinated carbonium ion, e.g.,

$$(CH_3)_3CH + H^+ \rightarrow \left[(CH_3)_3C^+\!\!<\!\!\begin{matrix}H\\H\end{matrix}\right] \rightarrow H_2 + (CH_3)_3C^+ \quad (3b)$$

It is shown herein that Reaction (3b) is unimportant with neopentane, which has only primary C–H bonds.

Several other possibilities have been suggested for the initiation step. (a) Trace amounts of olefins may provide a means of generating the initial carbenium ions. Several authors have reported the enhancement of the cracking and/or isomerization rate of paraffins after olefin addition (*4–9*). In a more acidic system, however, Magnotta and Gates (*10*) did not detect a rate enhancement upon addition of olefin. (b) Radical cations are known to form on the surface of aluminum silicates (*11*) and it has been suggested that these could be formed from molecules such as isobutane and then decompose to produce the olefins which enter the propagation steps (*12*). (c) The direct protonation of the paraffin has been suggested (*2, 13–15*) as pictured in Eqs. (3). (d) It has been claimed (*16*) that "neat" Lewis acids may insert into either a C–C or a C–H bond generating the carbenium ions. This possibility may be discounted on the basis of the results presented herein as well as on the long settled issue of the mechanism of formation of the $(C_6H_5)_3C^+$ from $(C_6H_5)_3CH$ where it was finally proved that Lewis acids were not responsible (*17*). On the other hand, the carbenium ion, once formed, may then follow the well-established chemistry of superacid solutions as described by Olah *et al.* (*18*).

In a recent publication Haag and Dessau (*15*) proposed the coexistence of two mechanisms, one represented by Eqs. (1) and (2) and the other by Eqs. (3) which depicts the C–H bond protonation. The latter mechanism was suggested to predominate at high temperatures and low pressures and conversions. It was deduced that varying contributions of these mechanisms occurred on silica–alumina, H–Y, and H–ZSM-5. In contrast with this controversial situation in heterogeneous catalysis, it is today widely accepted in liquid phase superacid chemistry (*18*) that the reactivity of the paraffins is due to the σ-donor ability of the shared electron pair of the C–H and C–C bonds of alkanes. These σ-bonds are able to form two electron three center bonds with an available proton, producing the pentacoordinated carbonium ions which then decompose into neutral molecules and tricoordinated carbenium ion.

The present work was initiated to clarify some of the controversial aspects of solid acid catalysis mentioned above. For this purpose a variety of solid acids of widely different acidity and pore sizes was selected. Neopentane (2,2-dimethylpropane) was chosen as a probe molecule since the insertion of H^+ for C–C cleavage should produce CH_4 and $(CH_3)_3C^+$ directly and β-scission is not possible. Neopentane is highly stable (*3*) and its chemistry in superacids is well known (*18, 19*). There is always a risk that mass transport effects may disguise the chemical processes occurring in small port molecular sieves (*20–23*). Tests indicated this not to be the case in the present work; these results will be reported later.

EXPERIMENTAL

Catalyst preparation and pretreatment. Davisil-623 silica gel and Houdry M-46 silica–alumina were obtained from commercial sources. The latter was taken from the same batch used in all of our earlier studies requiring such a catalyst.

Two samples of H–ZSM-5 were used. One was obtained from the Pittsburgh Energy Technology Center (PETC) and had a Si/Al ratio of 74. The other was a gift from Mobil Oil Corp. with a Si/Al ratio of 34.7. The Linde Y zeolite was dealuminated to match its Si/Al ratio with that of the very active slightly dealuminated mordenite.

TABLE 1

Physicochemical Properties of the Catalysts

	SiO_2	SiO_2–Al_2O_3	$AlCl_3/Al_2O_3$[a]	H–ZSM-5(74)	H–ZSM-5(35)	H–Y(8.1)	H–M(7.3)
Chemical Analysis							
SiO_2 (%)	99.7	87.5	—	98.8	97.6	90.2	88.7
Al_2O_3 (%)	—	12.5	99.9	1.13	2.4	9.3	10.1
(Al atoms/g) $\times 10^{-20}$	—	14.8	118	1.3	2.8	11.0	11.9
Si/Al (chemical)	—	5.9	—	74	34.7	8.1	7.3
Si/Al (framework)	—	—	—	74	35	13	11
Surface area (m^2/g)	340	270	192	—	—	—	—
Pore volume (cm^3/g)	1.2[b]	0.6[b]	0.8[b]	0.1[c] (0.18)	0.2[c] (0.18)	0.3[c] (0.3)	0.2[c] (0.2)
Brand name of starting material	Davisil-62 (W. R. Grace)	Houdry (M-46)	Ketjen-Al_2O_3 CK300	PETC	Mobil	Linde LZY62	Norton 2900H

[a] Data given for CK300.
[b] Pore volume given by the manufacturer.
[c] Calculated from oxygen saturation adsorption values; expected values from crystal structure are indicated in parentheses.

Thus, the extensive factor of the acidity of these two materials will be similar although the intensive factor may be very different. The starting material was a Linde LZY62 sieve (NH_4NaY) which was first exchanged twice with NH_4Cl to reduce the Na content. This sample was dealuminated following a standard procedure of hydrothermal treatment, then exchanged twice with NH_4NO_3, and followed by HCl extraction of the extra-lattice alumina (1.0 *N* HCl at 60°C for 2 h).

The H–mordenite was Norton Z900H with a Si/Al ratio of 5.9. It was refluxed for 2 h in 4 *M* HNO_3 and then thoroughly washed with deionized water. The physicochemical data of the catalysts are given in Table 1.

The $AlCl_3/Al_2O_3$ catalyst was prepared following the method described by Marczewski (*16*), which was slightly modified to exclude ambient air. The reactor was specially designed for this purpose. The U-tube reactor was modified by building on an extension separated by a breakable glass seal. The upper part was loaded with 0.4 g of γ-Al_2O_3 Ketjen CK-300 and the lower part with 0.1 g of anhydrous $AlCl_3$ research grade. This operation was carried out in a nitrogen glovebox and the lower extension sealed after loading the $AlCl_3$. The reactor was then connected to the high vacuum system and the alumina heat treated at 550°C, the same temperature as in (*16*), until an ultimate vacuum better than 10^{-5} Torr was obtained (within 4 h). Once this operation was completed the seal was broken and the $AlCl_3$ sublimed (at 200–250°C) onto the alumina. Finally the lower extension was sealed off and the catalyst was used in kinetic experiments without further treatment.

In preliminary runs pretreatments of the other catalysts in dried O_2 at 400 and 500°C were tested, but the reaction product distributions were not significantly different. Therefore, following the most often used treatment temperatures reported in the literature, all these catalysts were treated in flowing dried O_2 for 1 h at 500°C followed by evacuation to less than 10^{-5} Torr during another hour.

Reactants. High purity 2,2-dimethylpropane (99.9% + 0.1% isobutane) was used in these experiments. The He carrier gas was passed through a Matheson purifier and the hydrogen permeated through a silver–palladium alloy thimble; both gases tested pure to the parts per million range. These analyses were accomplished by collecting possible impurities from a metered flowing stream onto glass bead and silica gel traps

in series and both were thermostated at liquid nitrogen temperature. After a known (large) volume of gas had passed, the traps were warmed rapidly to room temperature or above and flushed by the same stream through a glc detector and measured in the usual fashion. Thus, the total impurity content could be estimated by dividing the volume of impurities recovered by the total gas passed.

Reaction procedure. The catalytic experiments were mostly performed in the pulse mode. However, the glass system also contained a recirculation loop equipped with a magnetic glass pump and could thus be operated in the stirred static mode. The glc system was calibrated by varying the pressure in the same doser used to measure the amount of reactant fed in each pulse. It had a calibrated volume of 1.57 cm^3. Products were trapped for 5 min at −195°C after passing the catalyst and then flashed onto the glc ($\frac{1}{4}$ in. by 10 ft 20% dibenzylamine on Chromosorb) column. CH_4 and H_2 if present were collected in a second trap packed with 5-Å sieves cooled in liquid nitrogen, placed after the glc detector (TCD). The methane was then measured in the same system while hydrogen was determined in another chromatograph. The fraction of reactant converted was calculated by dividing the sum of the micromoles of products obtained by glc (calculated as C_5) by the micromoles injected.

Residue (coke) measurements. These were made in the recirculation system using 200-Torr O_2 and with catalyst temperatures of 500°C. The CO_2 and H_2O were removed from the circulating gas in a U-loop trap cooled with liquid nitrogen. The CO_2 could be released at −78°C and the H_2O retained. Thus these gases could be separated and measured separately in a gas burette. After a given kinetic experiment the reactor was evacuated to $\sim 5 \times 10^{-5}$ Torr at the reaction temperature before admitting the oxygen.

RESULTS

Pulse Experiments

Tables 2 and 3 show the product distributions obtained when 1.54×10^{19} molecules in neopentane pulses were passed over 400

TABLE 2

Neopentane Cracking over Solid Acids (Conversion <5%)[a]

Molecules × 10^{-17}	SiO_2 (blank)[b]	SiO_2–Al_2O_3	$AlCl_3/Al_2O_3$	H–ZSM-5(74)	H–ZSM-5(35)	H–Y(8.1)	H–M(7.3)[c]
Reaction temperature (°C)	600	500	350	400	400	400	200
Conversion (%)	1.4	4.6	1.7	2.2	4.5	4.3	2.9
Neopentane converted	2.1	7.0	2.5	3.4	7.0	6.7	4.4
Methane	2.7	6.7	2.6	3.3	7.5	6.9	4.3
Ethane + Ethene	—	0.9	0.3	0.3	1.2	0.8	0.1
Propane	—	—	—	—	—	0.4	0.3
Propene	—	1.1	0.8	1.7	3.0	2.0	0.1
Isobutane	—	0.4	0.2	0.1	1.0	2.9	2.1
Isobutene	1.9	3.5	0.9	1.1	2.1	0.7	—
n-Butenes	—	1.9	0.7	0.9	0.9	0.4	—
Pentanes	—	—	—	—	—	0.2	—
C_4	1.9	5.8	1.8	2.0	4.0	4.1	2.1
$C_3 + C_4$	1.9	6.9	2.6	3.7	7.0	6.6	2.5
$P/Ol(C_3)$	—	0.0	0.0	0.0	0.0	0.2	4.6
$P/Ol(C_4)$	0	0.1	0.1	0.0	0.4	2.5	∞
$(C_2 + C_3)/C_4$	0	0.3	0.6	1.0	1.1	0.8	0.2
H/C (gas phase)	2.5	2.4	2.4	2.4	2.4	2.6	3.0

[a] Pulse reactor, 400 mg of catalyst, pulse size 1.54×10^{19} molecules. He carrier flow rate 90 cm^3/min.

[b] Free radical reactions in an empty quartz reactor give $CH_4/i\text{-}C_4H_8 = 1$ at $x = 1\%$; at higher conversions this ratio becomes greater than 1.

[c] These are data from first pulse. This catalyst showed pronounced deactivation with pulse number. Amount of residues measured after O_2 burning: CO_2, 8.1×10^{17} molecules; H_2O, 4.8×10^{17} molecules. The carbon analysis is equivalent to 1.6×10^{17} molecules of neopentane.

TABLE 3

Neopentane Cracking over Solid Acids (High Conversion)[a]

Molecules × 10^{-17}	SiO_2–Al_2O_3	$AlCl_3/Al_2O_3$	H–ZSM-5(74)[b]	H–ZSM-5(35)	H–Y(8.1)	H–M(7.3)[b]
Reaction temperature (°C)	600	450	500	500	450	250
Conversion (%)	47.8	40.0	32.0	45.2	25.5	36.4
Neopentane converted	73.6	61.6	49.2	69.7	39.3	49.5
Methane	85.3	69.2	54.1	84.1	47.2	49.6
Ethane + Ethene	7.3	8.1	8.2	36.9	6.2	0.9
Propane	—	0.5	0.2	4.1	5.5	5.4
Propene	9.9	17.9	20.2	33.8	9.0	0.5
Isobutane	3.4	2.8	1.1	4.3	18.5	23.0
Isobutene	34.7	24.6	15.4	8.8	2.6	—
n-Butenes	20.6	14.5	11.0	6.1	2.2	—
Pentanes[c]	—	—	—	—	0.1	1.1[d]
Pentenes	0.7	—	0.9	—	—	—
$C_3 + C_4$	68.6	60.2	47.9	57.1	37.8	28.9
$P/O(C_3)$	0	0.0	0.0	0.1	0.6	9.9
$P/O(C_4)$	0.1	0.1	0.0	0.3	3.9	∞
$(C_2 + C_3)/C_4$	0.3	0.6	1.0	3.9	0.9	0.3

[a] Reaction conditions see Table 1.
[b] Data from first pulse. Amount of residues equivalent to 15.9×10^{17} molecules of neopentane converted, included in third row.
[c] Mainly isopentane.
[d] Includes 0.11×10^{17} molecules of hexanes.

mg of catalyst in a purified He carrier gas stream (~90 cm^3/min). The results obtained at low conversion are shown in Table 2. The first column contains typical data (conversion level and product distribution) for a clean free radical mechanism. Note the close matching among the number of molecules converted, the amount of methane, and the total $C_3 + C_4$ produced for all the solid acids except the H–mordenite. In the latter case, the first two numbers were still very nearly equal because methane is formed in the primary step and the carbonaceous residue by secondary reactions of the *t*-butyl ion is released. Also note the growing importance of hydride transfer in going from left to right, as judged by the increasing paraffin to olefin ratios. These appear to follow the increase in activity with the possible exception of the $AlCl_3/Al_2O_3$ catalyst. Otherwise, this solid whose activity has been claimed to be due to the presence of Lewis sites (*16*) behaves just like all the other Brønsted acid catalysts. The products measured at high conversions (higher temperatures) show the same overall trends (Table 3).

Under the experimental conditions used, no mass loss due to residue formation could be determined chromatographically with any of the solid acids with the exception of H–mordenite. By combustion it was possible to measure the amount of residue left on all the catalysts after passage of ten pulses (at various temperatures). With H–Y(8.1), which formed more residue than any other catalyst except H–M, the total amount of neopentane converted in ten pulses was 38×10^{18} molecules while the total amount of residues produced was equivalent to 1×10^{18} molecules of neopentane. This is consistent with the inability to determine a mass loss from the glc analysis of individual pulses. Also consistent with this, the activity either remained constant or showed a slight tendency to increase with pulse number with the sole exception of the extremely active H–M sample which showed a steady decrease in activity.

The complete mass balance after passage of the first pulse over the mordenite catalyst is given in Table 4. The mass loss calculated from the chromatogram and from the amount of residues measured volumet-

TABLE 4

Mass Balance of Neopentane Reacting on H–Mordenite(7.3)

Fresh catalyst: 400 mg H–M (3.46×10^{20} Al)

Pulse of neopentane: 0.57 cm^3 = 1.54×10^{19} molecules

7.7×10^{19} C atoms

18.5×10^{19} H atoms

250°C

→ Residues[a]: CO_2 = 0.30 cm^3; H_2O = 0.13 cm^3; H/C = 0.86

Product	Molec. × 10^{-18}
C_5H_{12} converted	4.95
CH_4	4.96
C_2	0.09
C_3H_8	0.54
C_3H_6	0.05
i-C_4H_{10}	2.30
i-C_4H_8	—
η-C_4H_8	—
2MB (C_5H_{12})	0.11
C_6H_{14}	0.02
neo-C_5H_{12}	9.80

conversion to products and residues mol%: 36.36

C and H balance	C atoms × 10^{-18}	H atoms × 10^{-18}
Gaseous Products (rec.)	65.8	167.2
Residues	8.0	6.8
Total recovered:	73.8	174.1
Total injected:	77.1	185.0
Unaccounted	3.3 (4.3%)	10.9 (5.9%)

[a] Mass loss from volumetric measurements of CO_2 and H_2O formed on combustion was 9.2% and that determined from chromatograms was 8.4%.

rically as CO_2 and H_2O agreed within a few percent. The carbon and hydrogen mass balances showed an H/C ratio <1 in the residue and that about 5% of the reactant was not accounted for in the products. This latter result is probably within the experimental error of the techniques employed.

The fraction of neopentane converted to CH_4 when plotted vs $1000/T$ produced excellent straight lines as shown in Fig. 1. The experimental points were obtained going up and down in temperature at random. From the slopes of the lines drawn, the activation energies for methane formation were calculated and these values are shown in Fig. 1. Note the high activation energy obtained on the silica catalyst (free radical mechanism), the close similarity of the values calculated for silica–alumina and H–ZSM-5(74), and the much lower barriers observed on H–Y

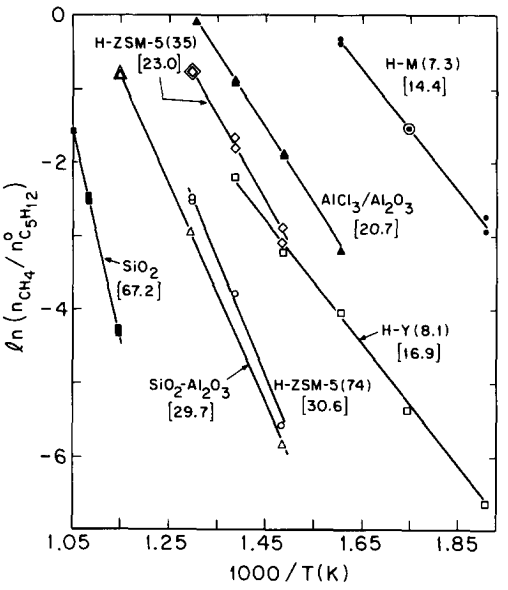

FIG. 1. Arrhenius plot of methane production. Numbers between parentheses indicate Si/Al ratios and those inside square brackets apparent activation energies in kilocalories per mole, ⧋, ◇, and ◉ indicate overlapping points.

and H–M. That for $AlCl_3/Al_2O_3$ lies between that for H–ZSM-5 and H–Y suggesting that the Brønsted sites on this preparation are stronger than those on M-46.

To obtain data at temperatures between 300 and 500°C on H–M(7.3) a reactor loaded with 40 mg was used instead of the usual 400-mg aliquots otherwise employed. Now the ratio of molecules per pulse to Al centers in the mordenite increased from 0.03 to 0.3. Under these circumstances the data points could not be reproduced due to rapid poisoning and for this same reason the apparent activation energy was now 10 ± 1 kcal/mol. This behavior is entirely consistent with the rapid deactivation reported below for the pulse and batch experiments conducted on the same catalyst (Table 5 and Fig. 2).

Pulse and batch experiments. To accelerate the deactivation process (coking) on mordenite, alternate pulse and batch experiments were made as shown in Table 5. As expected, there was a continuous decrease in activity with time of contact with the reactant. There were also more subtle changes in product distribution such as the decrease in methane production relative to the C_5H_{12} converted and the decrease in the C_3 paraffin/olefin ratio which may be taken as an index of the extent of hydrogen transfer. Isopentane, presumably formed by hydride abstraction of an H from neopentane, was clearly evident in this series of experiments. Also a gradual convergence of the (C_3 + C_4) molecules formed with the amounts of neopentane converted is seen. In the batch experiments, the sharp increase in C_3/C_4 ratio, when compared with the pulse experiments, demonstrates the increasing importance of secondary cracking.

A set of results obtained in the stirred static (batch) reactor is shown in Fig. 2. These will be helpful in deducing the over-

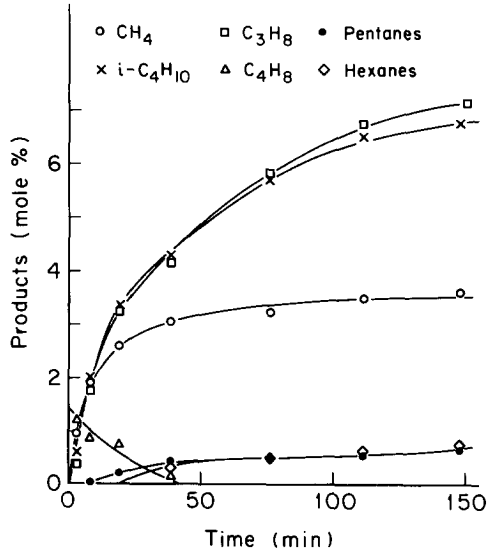

FIG. 2. Neopentane reactions on H–mordenite (Si/Al = 7.3). Batch, gas recirculation reactor (V = 455 cm³); reaction temperature, 250°C. Initial pressure, 250 Torr of neopentane. Amount of reactant, 37 × 10^{20} molecules. Amount of catalyst, 400 mg. Amount of residues after 150 min, CO_2 = 4.59 cm³, H_2O = 2.33 cm³, H/C = 0.97. The carbon analysis is equivalent to 2.5 × 10^{19} molecules of neopentane. At the end of run 86.5% of the reactant was still unconverted. The concentration of neopentane in the gas phase (not shown) steadily decreased along the run with diminishing slope.

TABLE 5

Deactivation of H–Mordenite(7.3)[a]

Molecules × 10^{-17}	Pulse 1	Batch 1[b]	Pulse 2	Pulse 3	Batch 2[c]	Pulse 4[d]
Amount of reactant	154	1351	154	154	1351	154
Conversion (%)	36.0	34.5	5.2	4.3	23.8	1.9
Neopentane converted	55.4	466	8.0	6.6	336	2.9
Methane	46.9	419	5.6	4.6	220	2.0
Ethene + Ethane	0.9	1.7	0.6	0.5	1.7	0.4
Propane	5.3	281.8	1.0	0.9	323	0.6
Propene	0.3	—	0.4	0.4	—	0.3
Isobutane (no butenes)	23.6	92.4	6.8	5.5	80.4	2.0
Isopentane	1.1	6.8	0.3	0.3	7.1	0.2
n-Pentane	—	3.6	—	—	3.3	—
Hexane	0.4	2.9	—	—	4.0	—
Residues (equiv. neo-C_5 molec.)	15.4[e]	126[f]	—	—	14[g]	—
C_3/C_4	0.2	3.1	0.2	0.2	4.0	0.5
$C_3 + C_4$	29.1	374.2	8.2	6.8	403.4	2.9
$P/Ol(C_3)$	21.1	∞	2.8	2.5	∞	1.8
C_6/C_5 converted × 10^3	0.8	0.6	—	—	1.2	—

[a] Reactant neopentane, reaction temperature 250°C; 400 mg H–M contains 4760 × 10^{17} Al atoms.

[b] Reaction time 10 min. P^0 = 250 Torr.

[c] Reaction time 50 min.

[d] Residues burnt in O_2 after this pulse. Amount of CO_2 = 2.9 cm^3, H_2O = 1.5 cm^3; H/C = 1.0.

[e] Estimated from chromatographic mass balance (consistent with Table 4).

[f] Estimated from chromatogram.

[g] Calculated as $d - (e + f)$.

all mechanistic picture of the reaction. The primary cracking reaction indexed by production of CH_4 was initially fast, but gradually virtually ceased. Secondary reactions went on as shown by the continuously increasing concentration of isobutane and propane. Measurable amounts of C_4 olefins appeared early in the reaction, but these disappeared as the reaction proceeded. During this experiment, which was carried out with a high reactant/catalyst ratio, the solid rapidly turned black and the reaction rate decreased sharply. This was also reflected in much larger amounts of residues formed (Fig. 2) compared with the pulse experiments (Table 4). These experiments demonstrated that the hydrogen required for paraffin production is furnished by these residues.

Effect of pre-reduction of the catalyst. From time to time it has been argued (*12*) that electron acceptor sites may be responsible for the initiation step in paraffin cracking by generating cation radicals. An experiment was made based upon previous studies of Dollish and Hall (*11*) who reported that radical ion formation from perylene or anthracene was severely diminished by reduction of the aluminum silicate (M-46 or H–Y) with H_2 at 500°C. In the present work H–ZSM-5 was used, based upon the claim of Shih (*24*) that such sites were identified on this material. The results reported in Table 6 show no important effect stemming from the reductive treatment. Neither the hydrogen reduction nor its use as carrier gas modified the activity or product distribution significantly in neopen-

TABLE 6

Effect of Hydrogen on Neopentane Conversion over H–ZSM-5[a]

Molecules × 10^{-17}	Pulse 1[b]	Pulse 2[c]	Pulse 3	Pulse 4[d]	Pulse 9[e]
Carrier	He	H_2	H_2	He	He
Conversion (%)	32.0	32.1	34.9	40.0	43.4
neo-C_5 converted	49.2	49.4	53.8	61.6	66.9
Methane	54.1	62.7	63.7	79.9	73.9
Ethane + Ethene	8.2	6.5	7.0	10.2	11.7
Propane	0.2	0.1	0.2	0.2	0.4
Propene	20.2	15.5	18.2	27.4	32.3
Isobutane	1.1	3.8	4.5	2.2	2.0
Isobutene	15.4	15.3	15.9	16.7	17.6
n-Butenes	11.0	10.9	11.8	11.6	13.6
Pentenes	0.9	0.9	0.9	0.7	1.3

[a] Pulse reactor; 400 mg of catalyst; pulse size, 0.57 cm^3. Both He and H_2 were flown at the same rate, 85 cm^3/min. Reaction temperature, 500°C.

[b] The catalyst was pre-reduced in flowing H_2 for 30 min.

[c] H_2 flow maintained for 30 min before sending Pulse 2.

[d] He flow maintained for 15 min before sending Pulse 4.

[e] This is Pulse 9 from another experiment in which He was used as carrier and the 8 previous pulses were either *n*-butane or neopentane and the reaction temperature varied between 250 and 500°C.

tane cracking. If anything, Table 6 shows a slow increase in activity independent of the type of carrier gas used, as was further documented by Pulse 9 taken from another experiment in which He was the only carrier gas used following treatment of the zeolite with flowing O_2. These results are inconsistent with the notion (*12*) that radical ions generated on electron acceptor sites play a significant role in paraffin cracking.

DISCUSSION

The present results clearly demonstrate that protonation of a C–C bond of neopentane by solid acids provides a route to initiate its decomposition. By analogy, the same route may generally initiate the formation of the first carbenium ions from paraffins which are necessary for cracking, hydride transfer, and all the other reaction characteristics of acid catalysis. The present data can most simply be described as follows.

On protonation, neopentane is decomposed into CH_4 and the *t*-butyl ion. The latter has a relatively long lifetime, but is in equilibrium with isobutene and the original Brønsted site. These are the primary reactions; secondary reactions follow. As olefins are formed, they react with other *t*-butyl ions on neighboring sites to form the expected C_8 carbenium ions which can rearrange by simple hydride and methyl shifts into isomeric ions. These can then cleave by β-scission forming C_5 olefins and the 2-propyl ion which being less stable desorbs as propene or, in the case of H–M, reacts with residues and desorbs as propane. The C_2 product can be accounted for in a similar way. Although some CH_4 may be produced by secondary protonation of the isobutane formed when this is a major product, the near equality between the methane formed and the neopentane reacted (at low conversions) suggests that this contribution is small (Table 2). Similarly, the isopentyl ion may be formed by hydride ion abstraction from neopentane (with concomitant rearrangement) by the primary *t*-butyl ion. The data suggest that with the possible excep-

tion of H–M, this process is relatively unimportant.

There are two properties which may be related to the intensive factor of the acidity (the strength of the acid–base interaction), viz., the activation energy required for methane formation (Fig. 1) and the position of the equilibrium

$$BH + CH_2{=}C(CH_3)_2 \rightleftarrows (CH_3)_3C^+ + B^- \quad (4)$$

The latter governs the lifetime of the carbenium ion, and hence, its propensity for secondary reactions, such as polymerization, rearrangement, and fragmentation, but most specifically hydride transfer (the paraffin/olefin ratios). Thus, neopentane reactions provide a useful tool for the evaluation of the acidic properties of catalysts.

From the above analysis a generalized reaction pathway may now be proposed for the cracking of neopentane over solid acids, which is also consistent with the known liquid phase chemistry of alkanes in superacids.

$$\text{neo-}C_5H_{12} + H^+ \rightarrow CH_4 + t\text{-}C_4H_9^+ \quad (5a)$$

$$\text{neo-}C_5H_{12} + H^+ \not\rightarrow H_2 + H_3C{-}\overset{\displaystyle CH_3}{\overset{|}{C^+}}{-}CH_2{-}CH_3 \quad (5b)$$

$$t\text{-}C_4H_9^+ + SiAlO^- \rightleftarrows i\text{-}C_4H_8 + SiAlOH \quad (4)$$

$$t\text{-}C_4H_9^+ + i\text{-}C_4H_8 \rightarrow \text{Oligomerization} \rightarrow \text{Rearrangement} + \beta\text{-scission} \quad (6)$$

$$\text{Oligomerization} \rightarrow \text{H-transfer} + \text{residues}$$

The introduction of Reaction (4) in this model merits further discussion. The product distribution will be affected by the interplay between the basicity of the intervening olefins and the strength of the solid acid. When the equilibrium is far to the right, olefins will desorb as the principal products, there being relatively few carbenium ions available with which to react. On the other hand, in the region where both are present, secondary reactions will become important. Unfortunately, little data are available on the basicity of olefins even in liquid phase, and hence a reliable measurement of the acid–base interaction energy on solid surfaces is still an unsolved problem. On one extreme of the acidity scale the basicity of isobutene in HF solution at 0°C has been measured by Hogeveen *et al.* (*25*): $[t\text{-}C_4H_9^+]/[i\text{-}C_4H_8] > 10^8$. On the other hand, Deno (*26*) provided a value for this ratio of 3×10^{-4} in 98% H_2SO_4. This indicates a fantastic variation in going from a superacid to a strong acid. The solid acids studied here may be fitted between these extremes. In fact, it has been previously suggested that H–mordenites show superacidity (*27*).

Indirect evidence was obtained on the variation of lifetime of the *t*-butyl carbenium ion with temperature. The paraffin/olefin C_4 ratios were measured at several temperatures. For H–M(7.3) at 250, 300, 350, and 400°C values of ∞, 65, 41, and 23, respectively, were obtained. This is consistent with the decreasing lifetime of the carbenium ion as the temperature is increased. These data demonstrate that comparisons of the different catalysts should be made at constant temperature. Under these circumstances, wide variations in rates of conversion are unavoidable (Fig. 1). However, the ratios obtained at 400°C were the following:

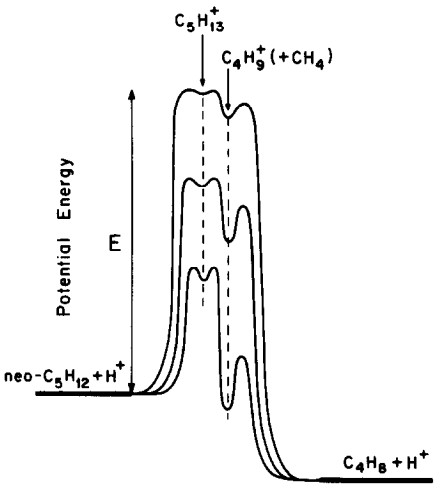

FIG. 3. Idealized reaction coordinates for neopentane decomposition on solid acids.

SiO_2/Al_2O_3 = 0.1, $AlCl_3/Al_2O_3$ = 0.1, H–ZSM-5(74) = 0.03, H–ZSM-5(35) = 0.4, H–Y(8.1) = 2.5 and H–M(7.3) = 23. Thus, the lifetime of the carbenium ion on the several surfaces would be expected to increase in the same order. Note that the same trend can be observed in the data of Tables 2 and 3.

Our product distributions can be readily rationalized in terms of Reactions (4)–(6). Reaction (5b) is negligible as shown by the relatively small amounts of either isopentene or isopentane formed. In a few selected experiments an attempt was made to detect the possible formation of H_2 without success (limit of detection in our system, 2×10^{17} H_2 molecules). This is consistent with the lower-electron donor capability of the primary C–H bond compared with the quaternary C–C bond (*18*). From the above discussion it can be inferred that the equilibrium in Reaction (4) is displaced toward the left in going from silica–alumina to H–M. This is also consistent with the decrease in activation energy between these two extreme cases recorded in Fig. 1.

The varying lifetime of the *t*-butyl carbenium ion may be schematically represented by the reaction coordinate scheme shown in Fig. 3. On solid acids such as silica–alumina or $AlCl_3/Al_2O_3$ the activation energy for carbonium ion formation is high (Fig. 1) and consequently the well corresponding to the metastable ion is shallow. In going to H–Y(8.1) and ultimately to H–M(7.3) this well gets deeper as the activation energy decreases and consequently the lifetime of the carbenium ion increases. It may even be that in the case of polymeric solid superacids this well becomes so deep that the ion becomes stable, i.e., lower in energy than the paraffin. Within this framework the H–mordenite will have the highest intensive factor and hence the lifetime of a given carbenium ion will be the longest on this surface. This in turn will make it more likely to react with other molecules, e.g., forming polymeric species on the surface (oligomerization) or produce paraffins by hydrogen transfer. As shown in Tables 4 and 5 and Fig. 2, abundant paraffins and residues are formed.

The discrepancies found in the literature about the promoting effects of olefins in the cracking of longer chain paraffins (see Introduction) may now be rationalized. With relatively weak acid catalysts Step 5 probably will be rate controlling. In this case the addition of olefins will assist in generating a useful population of carbenium ions on the surface and, hence, accelerate the reaction. With more acidic catalysts, e.g., the superacid polymers studied by Magnotta and Gates (*10*), the formation of the carbenium ions is not expected to be rate controlling and, hence, the rate should not be enhanced by introduction of small amounts of olefin into the stream as reported by them (*10*).

Haag and Dessau (*15*) were on the right track when they stated that two mechanisms coexist on H–ZSM-5, H–Y, and silica–alumina. Their "two mechanisms" included Reactions (4)–(6) and (1) and (2). It should be noted that larger molecules like *n*-hexane, after forming initial carbenium ions by Reaction (5), can undergo β-scission followed by H-transfer by Reactions (2) and (1), respectively.

An alternative interpretation, recently reiterated by Marczewski (*16*), envisions that Lewis acid sites play a direct role in the cracking of paraffins. This may be discounted by our results (Tables 2 and 3, and Fig. 1). On the one hand the product distribution obtained with $AlCl_3/Al_2O_3$ was indistinguishable from those obtained from silica–alumina or from H–ZSM-5. On the other hand, neither in our preparation nor in Marczewski's procedure can it be stated that Brønsted acids have been eliminated. It is well known that $AlCl_3$ can be activated to a strong Brønsted acid by traces of water, and γ-Al_2O_3 still retains a high concentration of hydroxyls after evacuation at 550°C (*28*) which can supply it. In brief, neither in heterogeneous nor in homogeneous superacid media (*18*) has it been possible to demonstrate that a "neat" Lewis acid (an electron acceptor site) is directly involved in a carbenium ion mechanism. Similarly, the H_2 reduction experiments demonstrate that the involvement of cation radicals is also highly unlikely.

Two final observations merit discussion. First, it has been frequently noted in the catalytic literature that mordenites coke very rapidly due to some structural characteristic, e.g., a slightly smaller pore entrance than Y zeolites or the unidimensional array of channels as compared with the three-dimensional interconnecting pore system of the faujasites. The data presented here suggest that the ultimate reason for the high rate of residue formation is the existence of very strong acid sites in H–mordenite which increase the lifetime of the ion and hence promote secondary reactions and hydrogen transfer in particular. Second, in view of the above, the ultimate differences in the behavior of H–ZSM-5 and silica–alumina may be the ability of the former structure to provide a single type of acid sites which are similar to the strongest ones in silica–alumina. This is an intriguing question that merits further research.

In summary, the use of neopentane cracking has served two main purposes. First, the existence of the proton insertion mechanism in heterogeneous acid catalyzed systems was demonstrated. This has been a much debated issue in the last few years. Second, a better understanding of the cracking mechanism has been obtained which has clarified some controversial results and views reported in the literature. This well-characterized reaction may be used as a probe to measure the acidity of many different solid acids.

ACKNOWLEDGMENT

We are grateful to Air Products and Chemicals, Inc. for supporting this work.

REFERENCES

1. Greensfelder, B. S., Voge, H. H., and Good, G. M., *Ind. Eng. Chem.* **41,** 2573 (1949).
2. Gates, B. C., Katzer, J. R., and Schuit, G. C. A., "Chemistry of Catalytic Processes." McGraw–Hill, New York, 1979.
3. Pines, H., "The Chemistry of Catalytic Hydrocarbon Conversions." Academic Press, New York, 1981.
4. Pines, H., and Wackter, R. C., *J. Amer. Chem. Soc.* **68,** 595 (1946).
5. Fejes, P., and Emmett, P. H., *J. Catal.* **5,** 193 (1966).
6. Pansing, W. F., *J. Phys. Chem.* **69,** 392 (1966).
7. Beyer, H., *Acta Chim. (Budapest)* **84,** 25 (1975).
8. Weisz, P., *Chem. Tech.*, 498 (1973).
9. Anufriev, D. M., Kuznetsov, P. N., and Ione, K. G., *J. Catal.* **65,** 221 (1980).
10. Magnotta, V. L., and Gates, B. C., *J. Catal.* **46,** 266 (1977).
11. Dollish, F., and Hall, W. K., *J. Phys. Chem.* **69,** 4402 (1965); Hall, W. K., *J. Catal.* **1,** 53 (1962).
12. McVicker, G. B., Kramer, G. M., and Ziemiak, J. J., *J. Catal.* **92,** 355 (1985).
13. Block, H. S., Pines, H., and Schmerling, L., *J. Amer. Chem. Soc.* **68,** 153 (1946).
14. Topchieva, K. V., *in* "Applications of Zeolites in Catalysis" (G. K. Boreskov and K. M. Minache, Eds.), p. 55. Akademiai Kiado, Budapest, 1979.
15. Haag, W. O., and Dessau, R. M., "Proceedings, 8th International Congress on Catalysis, Berlin, 1984," Vol. 2, p. 305. Dechema, Frankfurt-am-Main, 1984.
16. Marczewski, M., *J. Chem. Soc. Faraday Trans. 1* **82,** 1687 (1986).
17. Wu, C. Y., and Hall, W. K., *J. Catal.* **8,** 394 (1967).
18. Olah, G. A., Klopman, G., and Schlosberg, R. H., *J. Amer. Chem. Soc.* **91,** 3261 (1969); Olah, G. A.,

Surya, Prakash, G. K., and Sommer, J., "Superacids." Wiley, New York, 1985 (for an up-to-date review).

19. Olah, G. A., Halpern, Y., Shen, J., and Mo, Y. K., *J. Amer. Chem. Soc.* **95,** 4960 (1973).
20. Chen, N. Y., and Garwood, W. E., *J. Catal.* **52,** 453 (1978).
21. Frillette, V. J., Haag, W. O., and Lago, R. M., *J. Catal.* **67,** 218 (1981).
22. Haag, W. O., Lago, B. M., and Weisz, P. B., *Faraday Discuss.* **72,** 317 (1981).
23. Hilaireau, P., Bearez, Ch., Chevalier, F., Perot, G., and Guisnet, M., *Zeolites* **2,** 69 (1982).
24. Shih, S., *J. Catal.* **79,** 390 (1983).
25. Hogeveen, H., Gaasbeek, C. J., and Bickel, A. F., *Recl. Trav. Chim.* **88,** 703 (1969).
26. Deno, N. C., *Prog. Phys. Org. Chem.* **2,** 129 (1964).
27. Mirodatos, C., and Barthomcuf, D., *Chem. Commun.,* 39 (1981).
38. Millman, W. S., Crespin, M., Cirillo, A. C., Abdo, S., and Hall, W. K., *J. Catal.* **60,** 404 (1979).